TU Delft

Delft University of Technology

Reducing disorder in Ge quantum wells by using thick SiGe barriers

Costa, Davide; Stehouwer, Lucas E.A.; Huang, Yi; Martí-Sánchez, Sara; Degli Esposti, Davide; Arbiol, Jordi; Scappucci, Giordano

DOI
10.1063/5.0242746

Publication date
2024

Document Version
Final published version

Published in
Applied Physics Letters

Citation (APA)
Costa, D., Stehouwer, L. E. A., Huang, Y., Martí-Sánchez, S., Degli Esposti, D., Arbiol, J., & Scappucci, G. (2024). Reducing disorder in Ge quantum wells by using thick SiGe barriers. *Applied Physics Letters*, *125*(22), Article 222104. https://doi.org/10.1063/5.0242746

Important note
To cite this publication, please use the final published version (if applicable).
Please check the document version above.

Copyright
Other than for strictly personal use, it is not permitted to download, forward or distribute the text or part of it, without the consent of the author(s) and/or copyright holder(s), unless the work is under an open content license such as Creative Commons.

Takedown policy
Please contact us and provide details if you believe this document breaches copyrights.
We will remove access to the work immediately and investigate your claim.

This work is downloaded from Delft University of Technology.
For technical reasons the number of authors shown on this cover page is limited to a maximum of 10.

Applied Physics Letters

RESEARCH ARTICLE | NOVEMBER 26 2024

Reducing disorder in Ge quantum wells by using thick SiGe barriers

Davide Costa ; Lucas E. A. Stehouwer ; Yi Huang ; Sara Martí-Sánchez; Davide Degli Esposti ; Jordi Arbiol ; Giordano Scappucci

Check for updates

Appl. Phys. Lett. 125, 222104 (2024)
https://doi.org/10.1063/5.0242746

View Online
Export Citation

Articles You May Be Interested In

Germanium wafers for strained quantum wells with low disorder

Appl. Phys. Lett. (August 2023)

Sharp interface of undoped Ge/SiGe quantum well grown by ultrahigh vacuum chemical vapor deposition

Appl. Phys. Lett. (July 2022)

Lightly strained germanium quantum wells with hole mobility exceeding one million

Appl. Phys. Lett. (March 2022)

04 December 2024 15:16:03

AIP Publishing

Applied Physics Letters

Special Topics Open for Submissions

Learn More

AIP Publishing

Applied Physics Letters ARTICLE pubs.aip.org/aip/apl

Reducing disorder in Ge quantum wells by using thick SiGe barriers

Cite as: Appl. Phys. Lett. **125**, 222104 (2024); doi: 10.1063/5.0242746
Submitted: 7 October 2024 · Accepted: 15 November 2024 ·
Published Online: 26 November 2024

View Online Export Citation CrossMark

Davide Costa,[1] Lucas E. A. Stehouwer,[1] Yi Huang,[2] Sara Martí-Sánchez,[3] Davide Degli Esposti,[1] Jordi Arbiol,[3,4] and Giordano Scappucci[1,a)]

AFFILIATIONS

[1]QuTech and Kavli Institute of Nanoscience, Delft University of Technology, Lorentzweg 1, 2628 CJ Delft, Netherlands
[2]Condensed Matter Theory Center and Joint Quantum Institute, Department of Physics, University of Maryland, College Park, Maryland 20742, USA
[3]Catalan Institute of Nanoscience and Nanotechnology (ICN2), CSIC and BIST, Campus UAB, Bellaterra, 08193 Barcelona, Catalonia, Spain
[4]ICREA, Pg. Lluís Companys 23, 08010 Barcelona, Catalonia, Spain

[a)]Author to whom correspondence should be addressed: g.scappucci@tudelft.nl

ABSTRACT

We investigate the disorder properties of two-dimensional hole gases in Ge/SiGe heterostructures grown on Ge wafers, using thick SiGe barriers to mitigate the influence of the semiconductor–dielectric interface. Across several heterostructure field effect transistors, we measure an average maximum mobility of $(4.4 \pm 0.2) \times 10^6$ cm^2/Vs at a saturation density of $(1.72 \pm 0.03) \times 10^{11}$ cm^{-2}, corresponding to a long mean free path of $(30 \pm 1)\mu$m. The highest measured mobility is 4.68×10^6 cm^2/Vs. We identify uniform background impurities and interface roughness as the dominant scattering mechanisms limiting mobility in a representative device, and we evaluate a percolation-induced critical density of $(4.5 \pm 0.1) \times 10^9$ cm^{-2}. This low-disorder heterostructure, according to simulations, may support the electrostatic confinement of holes in gate-defined quantum dots.

© 2024 Author(s). All article content, except where otherwise noted, is licensed under a Creative Commons Attribution-NonCommercial-NoDerivs 4.0 International (CC BY-NC-ND) license (https://creativecommons.org/licenses/by-nc-nd/4.0/). https://doi.org/10.1063/5.0242746

04 December 2024 15:16:03

Holes confined in strained Ge quantum wells are a promising platform for quantum computation with gate-defined quantum dots.[1] Beneficially, the low effective mass[2,3] allows the definition of quantum dots using large electrodes[4] and the sizeable spin–orbit coupling enables local qubit control that is fully electrical and fast.[5] Recent progress in size and functionality of planar Ge qubit devices include the shared control of a 16 semiconductor quantum dot crossbar array,[6] a four qubit germanium quantum processor,[7] singlet-triplet qubits at low magnetic fields,[8] sweet-spot qubit operation,[9] and hopping-based universal quantum logic.[10] All these demonstrations used Si as a substrate for the growth of Ge/SiGe heterostructures. Previous work[11] has shown how moving from Si to Ge wafers, however, enables better Ge-rich SiGe strain-relaxed buffers (SRBs) because of the smaller lattice mismatch between substrate and strained Ge quantum well. These SRBs on a Ge wafer have a low threading dislocation density of $(6 \pm 1) \times 10^5$ cm^{-2}, nearly one order of magnitude improvement compared to control SRBs on Si wafers.[12] The associated reduction in short range scattering allows for an improvement of the electrical performance of the two-dimensional hole gas (2DHG) in the quantum well, reaching a mobility of $(3.4 \pm 0.1) \times 10^6$ cm^2/Vs.[11] In this Letter, we further explore the potential of Ge/SiGe heterostructures on Ge wafers by growing a thicker SiGe barrier to mitigate disorder from the semiconductor–dielectric interface. By combining Hall transport measurements and scattering theory, we demonstrate an improved mobility and percolation density, setting a benchmark for group IV semiconductors, whilst giving insights into the remaining sources of disorder. Schrödinger–Poisson simulations of quantum confined energy levels indicate that this heterostructure is suitable for hosting gate-defined hole quantum dots.

We grow a Ge/SiGe heterostructure on a Ge wafer by reduced-pressure chemical vapor deposition, following the same growth protocol described in Ref. 11. The epitaxial stack comprises a $Si_{0.17}Ge_{0.83}$ SRB by step grading, a compressively strained Ge quantum well, and a $Si_{0.17}Ge_{0.83}$ barrier passivated by a thin Si cap. Here, we increase the $Si_{0.17}Ge_{0.83}$ barrier thickness from 55 to 135 nm.[11] We fabricate Hall-bar shaped heterostructure field effect transistors (H-FETs) for

© Author(s) 2024

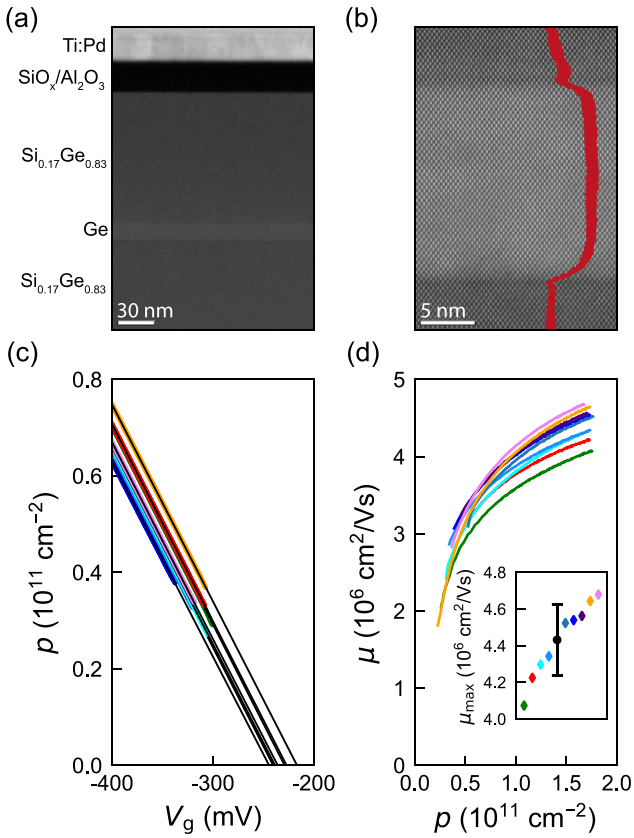


FIG. 1. (a) HAADF-STEM image of the active layers of the Ge/SiGe heterostructure field effect transistor. The 16 nm strained Ge quantum well is grown coherently on a $Si_{0.17}Ge_{0.83}$ strain-relaxed buffer. A 135 nm $Si_{0.17}Ge_{0.83}$ barrier separates the quantum well from the dielectric stack. The dielectric stack comprises a thin native silicon oxide layer followed by a 30 nm Al_2O_3 film obtained by atomic layer deposition at 300 °C. (b) Close-up image of the Ge quantum well with a superimposed average of the intensity profile (red curve). (c) Hall density p as a function of gate voltage V_g for 9 heterostructure field effect transistors from the same wafer (colored lines) and corresponding linear fits (black lines). (d) Hole mobility μ as a function of Hall density p for the same heterostructure field effect transistors (colored lines) and distribution of maximum mobility μ_{max} (inset). Maximum mobility from all the devices (diamonds), average value, and standard deviation (black) are shown.

magnetotransport characterization by four-probe low-frequency lock-in techniques, as described in Ref. 12. Figure 1(a) shows a high angle annular dark field (HAADF) scanning transmission electron microscopy (STEM) image of the active layers of the H-FET, with no visible defects or dislocation. From the image in Fig. 1(b), we estimate a quantum well width $w = 16$ nm and a characteristic length-scale 4τ of both the top and bottom interface of 2 nm, by fitting the intensity profile to a sigmoid model[13,14] (see the supplementary material). However, the applicability of this model may be limited since we observe a slight accumulation of Si (or depletion of Ge) at both top and bottom interfaces of the quantum well, manifesting as darker lines in the HAADF-STEM image and therefore dips in the contrast profile.

We characterize disorder in this heterostructure by magnetotransport measurements across nine H-FETs in a dilution refrigerator equipped with a cryo-multiplexer[15] (temperature $T = 100$ mK measured at the mixing chamber). Applying a negative gate voltage V_g capacitively induces a 2DHG and controls the carrier density p in the quantum well as shown in Fig. 1(c). From the observed linear p–V_g relationships, we obtain a capacitance per unit area C of (65.5 ± 0.3) nF/cm^2 averaged across the H-FETs. The very small standard deviation (less than 0.5%) indicates highly uniform thickness and dielectric properties of the SiGe barrier and the SiO_2/Al_2O_3 layer on top. Furthermore, we extract the gate voltages V_0 for which the density extrapolates to zero [Fig. 1(c), black solid lines] and obtain an average value of (-233.8 ± 8.4) mV. Since C is uniform throughout the devices, the tight distribution of V_0, with a standard deviation of 3.6%, is an indication of the very low disorder of the electrostatic potential landscape in the channel. Figure 1(d) shows the density-dependent mobility μ. Whilst all devices achieve a similar saturation density p_{sat} of $(1.72 \pm 0.03) \times 10^{11}$ cm^{-2}, which is consistent with the uniform C, we do observe differences in the lowest measurable Hall density, which is 2.27×10^{10} cm^{-2} for the orange curve. These differences might arise from different contact resistances at low density across the devices. As a general trend, the mobility increases over the whole range of investigated density for all H-FETs. We observe a maximum mobility of $(4.4 \pm 0.2) \times 10^6$ cm^2/Vs averaged across the 9 H-FETs [Fig. 1(d), inset] and measured at p_{sat}, corresponding to an average mean free path of $(30 \pm 1)\mu$m. The largest mobility measured within the distribution is 4.68×10^6 cm^2/Vs, which represents a 9% improvement over the previously highest reported hole mobility in Ge/SiGe heterostructures,[16] setting a benchmark for group IV semiconductors. While the heterostructures in Ref. 16 had a dislocation density twice as high, in the 10^6 cm^{-2} range, from being grown on a Si wafer, they exhibited less Si–Ge interdiffusion in the active region

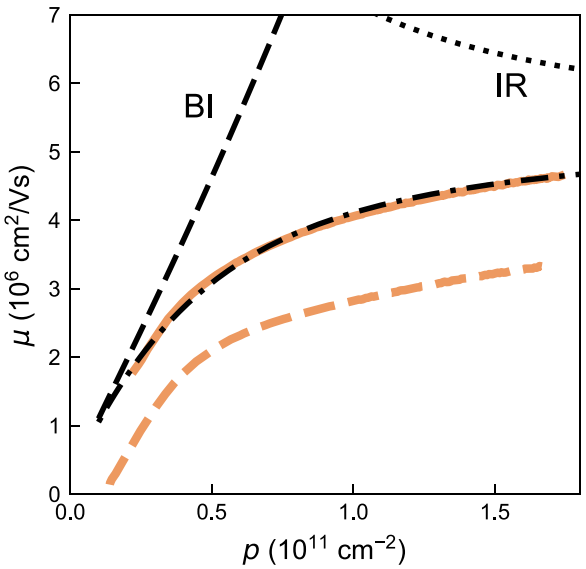


FIG. 2. Mobility μ as a function of density p from a representative heterostructure field effect transistor with a 135 nm thick SiGe barrier. The dashed-dotted black curve is a theoretical fit to the data considering scattering from a uniform background of charged impurities (BI) and interface roughness (IR). The individual contributions from BI and IR are shown as a dashed black curve and a dotted black curve, respectively. The dashed orange curve is from a similar heterostructure with a thinner SiGe barrier of 55 nm.[11]

04 December 2024 15:16:03

© Author(s) 2024

possibly due to a lower growth temperature (below 500 °C) compared to our heterostructures.

To gain insights into the scattering mechanisms in these high-mobility strained Ge quantum wells, we analyze in Fig. 2 the mobility-density curve from the H-FET with the largest measured density range [orange curve, also plotted in Fig. 1(d)]. We use Boltzmann transport theory at $T = 0$ K and calculate the mobility of the 2DHG in the Born approximation, taking into account the wavefunction of a finite potential well, the gate screening effect, and the local field correction following Ref. 17 (see the supplementary material). The fit to the theory (dashed-dotted black curve) shows good agreement with the experimental data and was calculated considering the contribution to the scattering rate from both uniform background charged impurities (BI) and interface roughness (IR). These individual contributions are shown as dashed black lines (BI) and dotted black lines (IR) in Fig. 2, and were obtained using a background impurity concentration of $N_b = 3.8 \times 10^{13}$ cm^{-3} and a surface roughness characterized by a typical height of $\Delta = 10$ Å and lateral size of $\Lambda = 28$ Å. To investigate how relevant is the disorder induced by the semiconductor–dielectric interface, we further evaluate the scattering rate contributed by remote charged impurities (RI). The mobility limited by RI has a quasi-cubic dependence (see the supplementary material) with the distance between the semiconductor–dielectric interface and the 2DHG in the quantum well, which is approximated by the SiGe barrier thickness. This suggests that if RI were the dominant scattering mechanism, increasing the barrier thickness from 55 nm (dashed orange line, from Ref. 11) to 135 nm (solid orange line) would result in more than one order of magnitude increase in mobility. However, the mobility increased by a factor of ≈ 1.6, from which we conclude that the dominant scattering mechanisms for this H-FET with a thick SiGe barrier are BI at low density and IR at high density, respectively.

We further investigate disorder in the low-density regime by analyzing, for the same H-FET, the density-dependent conductivity σ_{xx} to determine the percolation density p_p. The common method of extracting p_p is to fit the longitudinal conductivity σ_{xx} to the relationship $A(p - p_p)^{\alpha}$,[18,19] with coefficient A and p_p as fitting parameters[20] and exponent α fixed to the theoretical value of 1.31 from percolation theory in 2D.[21] Two aspects of fitting percolation density, however, require attention: first, there are studies that consider the exponent α as a free fitting parameter.[16,22] Second, since the theory is only valid in the low-density regime around p_p, a meaningful estimate of p_p should account for its dependence on the density range Δp over which the fit is performed.[23,24] We systematically address these aspects by performing the following series of percolation fits: for a given value of α, we fix the lower boundary of Δp to the minimum measured Hall density of 2.27×10^{10} cm^{-2} and gradually increase the upper bound until it encompasses the full range under consideration.

We assess the quality of the obtained percolation fits using the R-squared method and in Fig. 3(a) show $\log(1 - R^2)$ across the portion of the $\alpha - \Delta p$ plane investigated. The local minima are positioned along a continuous curve $\vec{s}(\alpha, \Delta p)$ (white dashed line), which identifies the region of best fit to the experimental data and crosses the theoretical 2D case of $\alpha = 1.31$ at a low $\Delta p = 2 \times 10^{10}$ cm^{-2} (red circle). In Fig. 3(b), we show the obtained p_p values across the $\alpha - \Delta p$ plane and we use the curve $\vec{s}(\alpha, \Delta p)$ to refine the selection of p_p for a more reliable evaluation. The corresponding p_p values are shown in Fig. 3(c) as a function of displacement $\Delta\vec{s}$ along $\vec{s}(\alpha, \Delta p)$ and relative to the

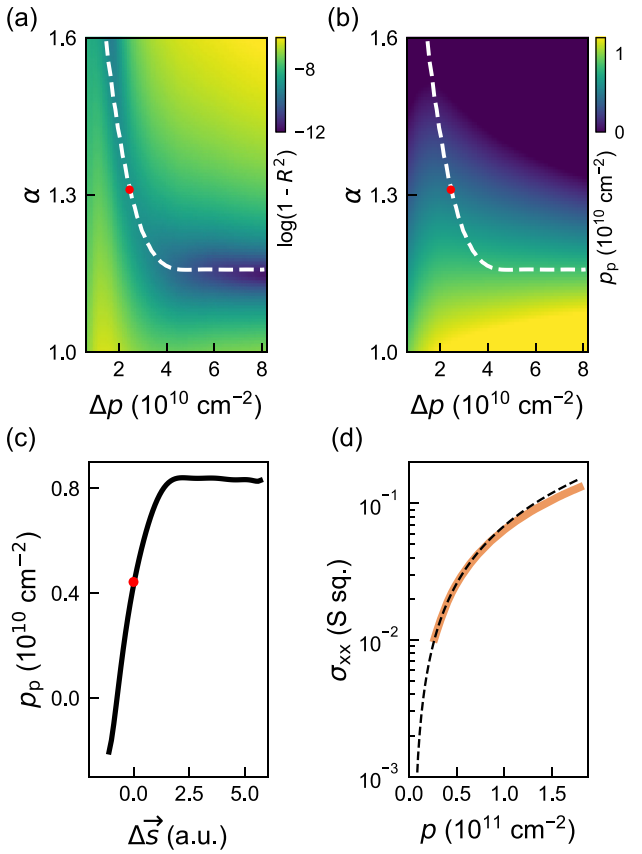


FIG. 3. (a) Map of $\log(1 - R^2)$ as a function of variables α and Δp, where R^2 is the coefficient of determination obtained by fitting the density-dependent conductivity $\sigma_{xx}(p)$ from the device in Fig. 2 to the theoretical model $A(p - p_p)^{\alpha}$. Both A and the percolation density p_p are free fitting parameters, while Δp is the density range over which the data are fitted, starting from the minimum measured density. The dashed white curve $\vec{s}(\alpha, \Delta p)$ follows the local minima of $\log(1 - R^2)$. For $\alpha = 1.31$, which is the critical exponent expected from percolation theory in 2D, the local minimum is found at $\Delta p = 2 \times 10^{10}$ cm^{-2} (red dot). (b) Corresponding map of the fitted p_p as a function of α and Δp, with superimposed dashed white curve $\vec{s}(\alpha, \Delta p)$ and red dot as in (a). (c) Values of p_p as a function of the displacement $\Delta\vec{s}$ along the curve $\vec{s}(\alpha, \Delta p)$, relative to the position of the red dot. (d) Experimental $\sigma_{xx}(p)$ curve (orange) and best fit to percolation theory in 2D (dashed black line). α and Δp are fixed to the values identifying the red dot in (a).

position of best fit for the theoretical 2D case (red circle). The fitted p_p shows an upper bound of about 8.5×10^9 cm^{-2} for positive $\Delta\vec{s}$ at $\alpha = 1.15$, whereas for negative displacements $\Delta\vec{s}$, i.e., $\alpha > 1.31$, p_p may become arbitrarily small, and even take negative, and therefore unphysical, values for $\alpha > 1.5$. For the 2D theoretical case of a percolation-induced metal–insulator transition, characterized by a fixed universal exponent $\alpha = 1.31$, p_p assumes a value of $(4.5 \pm 0.1) \times 10^9$ cm^{-2}, with the experimental data and corresponding very good fit shown as a reference in Fig. 3(d).

Having demonstrated the merits of a thick SiGe barrier for obtaining a very low-disordered 2DHG, we now assess the practicality of this design choice for confining holes in gate-defined quantum dots. We perform 2D Schrödinger–Poisson simulations using the NEXTNANO software package and show in Fig. 4(a) the edge of the first heavy-hole

04 December 2024 15:16:03

© Author(s) 2024

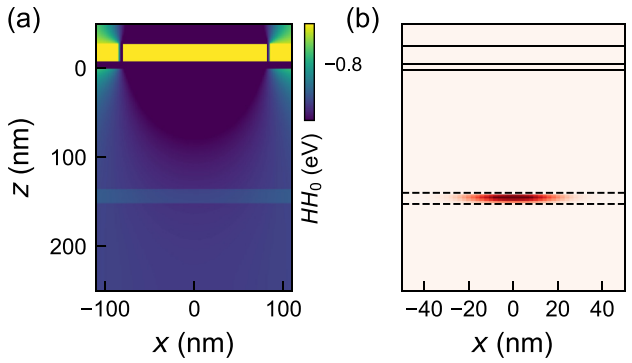


FIG. 4. (a) Simulated ground state heavy-hole (HH) band edge (HH_0) as a function of the x and z coordinates. The strained Ge quantum well is positioned 135 nm below the gate stack ($z < 0$). The plunger gate and the barrier gates are 160 and 30 nm wide, respectively. All gates are 30 nm thick. (b) Hole population of the HH ground state, showing a quantum dot-like confinement.

band (HH_0). The top interface of the quantum well is positioned at $z = 135$ nm and the gate stack (a plunger and two barrier gates with dielectric in between) is visible for $z < 0$ nm. Following calculations of the confined energy levels for the heavy-hole and light-hole states, we show in Fig. 4(b) that under appropriate voltages applied to the gates (−0.58 V and −0.4 V for plunger and barriers, respectively), only the first heavy-hole state is occupied in the quantum well. This supports the feasibility of fabricating quantum dots on this heterostructure.

In summary, we investigate Ge/SiGe heterostructures on Ge wafers and demonstrate an improved disorder in the Ge quantum well by using a thick SiGe barrier. The electrical performance of the 2DHG is limited by uniform background impurities and interface roughness and shows very high mobility and low percolation density, which we assessed with a critical evaluation of the fitting procedure. Additional insights into the structural and electrical properties of the heterostructure may be gained by using electron tomography to reconstruct the quantum well interface roughness and alloy disorder in three dimensions,[25] and by evaluating the single-particle lifetime and quantum mobility[26] from magnetotransport measurements. The high mobility reported recently in Ge/SiGe heterostructures with similar SiGe barrier thickness and alloy composition,[16] despite their higher dislocation density as they were grown on a Si wafer, is very encouraging. These results suggest that much further improvement in the Ge/SiGe heterostructure on Ge wafers could be also achieved by purifying both Si and Ge gas precursors to suppress background contamination and by eventually lowering the growth temperature of the quantum well and barriers below 500 °C to suppress the Si and Ge interdiffusion at the quantum well interfaces. We predict that quantum confinement of holes in gate-defined quantum dots is feasible in this heterostructure and we estimate that dots of about $1/\sqrt{p_p} \approx 150$ nm in size, informative about the average distance between impurities or other traps, could be essentially disorder-free. On the path to better performing spin-qubits, further measurements of charge noise in quantum dots will give insights into the dynamics of charge fluctuations that are not probed by magnetotransport experiments.

See the supplementary material for fits of the intensity profile from the electron microscope images, notes on scattering theory for germanium quantum wells and conductivity–density curves for all measured H-FETs.

We acknowledge Sankar Das Sarma for fruitful discussions. This work was supported by the Netherlands Organization for Scientific Research (NWO/OCW), via the Frontiers of Nanoscience program and a Projectruimte program. This research was supported by the European Union's Horizon 2020 research and innovation programme under the Grant Agreement Nos. 951852 and 101069515. This research was sponsored in part by The Netherlands Ministry of Defence under Award No. QuBits R23/009. The theoretical work for fitting of the mobility–density curves was supported by LPS, Laboratory of Physical Sciences. ICN2 acknowledges funding from Generalitat de Catalunya 2021SGR00457. ICN2 is supported by the Severo Ochoa program from Spanish MCIN/AEI (Grant No. CEX2021-001214-S) and is funded by the CERCA Programme/Generalitat de Catalunya and ERDF funds from EU. We acknowledge support from CSIC Interdisciplinary Thematic Platform (PTI+) on Quantum Technologies (PTI-QTEP+). The views, conclusions, and recommendations contained in this document are those of the authors and are not necessarily endorsed nor should they be interpreted as representing the official policies, either expressed or implied, of The Netherlands Ministry of Defence. The Netherlands Ministry of Defence is authorized to reproduce and distribute reprints for Government purposes notwithstanding any copyright notation herein.

AUTHOR DECLARATIONS

Conflict of Interest

The authors have no conflicts to disclose.

Author Contributions

Davide Costa: Data curation (lead); Methodology (equal); Visualization (lead); Writing – original draft (equal); Writing – review & editing (equal). **Lucas E. A. Stehouwer:** Methodology (equal); Writing – review & editing (equal). **Yi Huang:** Formal analysis (equal); Methodology (equal); Writing – review & editing (equal). **Sara Marti-Sanchez:** Formal analysis (equal); Methodology (equal); Writing – review & editing (equal). **Davide Degli Esposti:** Formal analysis (equal); Writing – review & editing (equal). **Jordi Arbiol:** Methodology (equal); Supervision (equal); Writing – review & editing (equal). **Giordano Scappucci:** Funding acquisition (lead); Supervision (lead); Writing – original draft (equal); Writing – review & editing (equal).

DATA AVAILABILITY

The data that support the findings of this study are openly available in 4TU Research Data at https://doi.org/10.4121/a4fce2ed-262f-4db9-866b-661c0e002671, Ref. 27.

REFERENCES

[1]G. Scappucci, C. Kloeffel, F. A. Zwanenburg, D. Loss, M. Myronov, J.-J. Zhang, S. De Franceschi, G. Katsaros, and M. Veldhorst, Nat. Rev. Mater. **6**, 926 (2020).

04 December 2024 15:16:03

© Author(s) 2024

[2]M. Lodari, A. Tosato, D. Sabbagh, M. A. Schubert, G. Capellini, A. Sammak, M. Veldhorst, and G. Scappucci, Phys. Rev. B **100**, 041304 (2019).
[3]L. A. Terrazos, E. Marcellina, Z. Wang, S. N. Coppersmith, M. Friesen, A. R. Hamilton, X. Hu, B. Koiller, A. L. Saraiva, D. Culcer, and R. B. Capaz, Phys. Rev. B **103**, 125201 (2021).
[4]W. Lawrie, H. Eenink, N. Hendrickx, J. Boter, L. Petit, S. Amitonov, M. Lodari, B. Paquelet Wuetz, C. Volk, S. Philips *et al.*, Appl. Phys. Lett. **116**, 080501 (2020).
[5]N. Hendrickx, D. Franke, A. Sammak, G. Scappucci, and M. Veldhorst, Nature **577**, 487 (2020).
[6]F. Borsoi, N. W. Hendrickx, V. John, M. Meyer, S. Motz, F. van Riggelen, A. Sammak, S. L. de Snoo, G. Scappucci, and M. Veldhorst, Nat. Nanotechnol. **19**, 21 (2024).
[7]N. W. Hendrickx, W. I. Lawrie, M. Russ, F. van Riggelen, S. L. de Snoo, R. N. Schouten, A. Sammak, G. Scappucci, and M. Veldhorst, Nature **591**, 580 (2021).
[8]D. Jirovec, A. Hofmann, A. Ballabio, P. M. Mutter, G. Tavani, M. Botifoll, A. Crippa, J. Kukucka, O. Sagi, F. Martins *et al.*, Nat. Mater. **20**, 1106 (2021).
[9]N. Hendrickx, L. Massai, M. Mergenthaler, F. Schupp, S. Paredes, S. Bedell, G. Salis, and A. Fuhrer, Nat. Mater. **23**, 920–927 (2024).
[10]C.-A. Wang, V. John, H. Tidjani, C. X. Yu, A. S. Ivlev, C. Déprez, F. van Riggelen-Doelman, B. D. Woods, N. W. Hendrickx, W. I. Lawrie *et al.*, Science **385**, 447 (2024).
[11]L. E. Stehouwer, A. Tosato, D. Degli Esposti, D. Costa, M. Veldhorst, A. Sammak, and G. Scappucci, Appl. Phys. Lett. **123**, 092101 (2023).
[12]A. Sammak, D. Sabbagh, N. W. Hendrickx, M. Lodari, B. Paquelet Wuetz, A. Tosato, L. Yeoh, M. Bollani, M. Virgilio, M. A. Schubert *et al.*, Adv. Funct. Mater. **29**, 1807613 (2019).
[13]B. Paquelet Wuetz, M. P. Losert, S. Koelling, L. E. A. Stehouwer, A.-M. J. Zwerver, S. G. J. Philips, M. T. Mądzik, X. Xue, G. Zheng, M. Lodari, S. V. Amitonov, N. Samkharadze, A. Sammak, L. M. K. Vandersypen, R. Rahman, S. N. Coppersmith, O. Moutanabbir, M. Friesen, and G. Scappucci, Nat. Commun. **13**, 7730 (2022).
[14]D. Degli Esposti, L. E. Stehouwer, Ö. Gül, N. Samkharadze, C. Déprez, M. Meyer, I. N. Meijer, L. Tryputen, S. Karwal, M. Botifoll *et al.*, npj Quantum Inf. **10**, 32 (2024).
[15]B. Paquelet Wuetz, P. Bavdaz, L. Yeoh, R. Schouten, H. Van Der Does, M. Tiggelman, D. Sabbagh, A. Sammak, C. G. Almudever, F. Sebastiano *et al.*, npj Quantum Inf. **6**, 43 (2020).
[16]M. Myronov, J. Kycia, P. Waldron, W. Jiang, P. Barrios, A. Bogan, P. Coleridge, and S. Studenikin, Small Sci. **3**, 2200094 (2023).
[17]Y. Huang and S. D. Sarma, Phys. Rev. B **109**, 125405 (2024).
[18]B. J. Last and D. J. Thouless, Phys. Rev. Lett. **27**, 1719 (1971).
[19]B. I. Shklovskiĭ and A. L. Éfros, Sov. Phys. Usp. **18**, 845 (1975).
[20]L. Tracy, E. Hwang, K. Eng, G. Ten Eyck, E. Nordberg, K. Childs, M. Carroll, M. Lilly, and S. D. Sarma, Phys. Rev. B **79**, 235307 (2009).
[21]R. Fogelholm, J. Phys. C **13**, L571 (1980).
[22]J.-S. Kim, A. M. Tyryshkin, and S. A. Lyon, Appl. Phys. Lett. **110**, 123505 (2017).
[23]M. Lodari, N. W. Hendrickx, W. I. Lawrie, T.-K. Hsiao, L. M. Vandersypen, A. Sammak, M. Veldhorst, and G. Scappucci, Mater. Quantum Technol. **1**, 011002 (2021).
[24]D. Sabbagh, N. Thomas, J. Torres, R. Pillarisetty, P. Amin, H. George, K. Singh, A. Budrevich, M. Robinson, D. Merrill *et al.*, Phys. Rev. Appl. **12**, 014013 (2019).
[25]E. Paysen, G. Capellini, E. Talamas Simola, L. Di Gaspare, M. De Seta, M. Virgilio, and A. Trampert, ACS Appl. Mater. Interfaces **16**, 4189 (2024).
[26]S. D. Sarma and E. H. Hwang, Phys. Rev. B **90**, 035425 (2014).
[27]D. Costa and G. Scappucci (2024). "Data Repository for 'Reducing disorder in Ge quantum wells by using thick SiGe barriers,'" 4TU.ResearchData. Dataset https://doi.org/10.4121/a4fce2ed-262f-4db9-866b-661c0e002671

04 December 2024 15:16:03

© Author(s) 2024